

Probing Pseudoscalars with Pulsar Polarisation Data Sets

Karam Chand^a, Subhayan Mandal^a

^a*Physics Department, Malaviya National Institute Of Technology, Jaipur, Rajasthan-302017, India*

e-mail addresses: 2015rpy9054@mnit.ac.in, smandal.phy@mnit.ac.in

November 9, 2018

Abstract

Recently a data set containing linear and circular polarisation information of a collection of six hundred pulsars has been released. The operative radio wavelength for the same was 21 cm. Pulsars radio emission process is modelled either with synchrotron / superconducting self-Compton route or with curvature radiation route. These theories fall short of accounting for the circular polarisation observed, as they are predisposed towards producing, solely, linear polarisation. Here we invoke (pseudo)scalars and their interaction with photons mediated by colossal magnetic fields of pulsars, to account for the circular part of polarisation data. This enables us to estimate the pseudoscalar parameters such as its coupling to photons and its mass in conjunction as product. To obtain these values separately, we turn our attention to recent observation on 47 pulsars, whose absolute polarisation position angles have been made available. Except, a third of the latter set, the rest of it overlaps with the expansive former data set on polarisation type & degree. This helps us figure out, both the pseudoscalar parameters individually, that we report here.

1 Introduction

In the last two decades, scenarios in which pseudoscalar [1–6] particles and photons couple and subsequently mix (fig no. 1) in the presence of magnetic fields have received a lot of attention [7–13], both phenomenologically [14–21] and observationally [22–29]. This is of particular interest in astrophysics, where this mixing of photons with pseudoscalars could make the universe transparent [30], change the polarisation properties of light [31] and is potentially responsible for effects such as Supernovae dimming [30] or Large-scale coherent orientation [31] of the universe, also known as ‘Hutsemekers’ effect. The best-known light pseudoscalar particle, the axion, was introduced long ago [32] to explain the absence of CP violation in Quantum Chromodynamics (QCD) [33]. One postulated the existence of a new spontaneously broken continuous Peccei-Quinn symmetry, so that the axion was a pseudo Goldstone boson. It was soon realised that one needed to introduce a very large scale in the theory in order to suppress the interactions of the axion, while preserving the Peccei-Quinn mechanism. The invisible axion [34] emerges at a unification scale, and the effective coupling is suppressed by this scale. The invisible axion, being closely related to QCD, has definite and interrelated expressions for its mass [35] and coupling strength [36] to other particles, given a specific model [37, 38]. Various cosmological and astrophysical bounds can be used to further constrain the parameters [36], and the allowed parameters do not lead to observable effects over cosmological scales. The mass of the pseudoscalar particle needs to be very close to the photon effective mass in order to mix in the rather weak magnetic fields of the extra galactic space. However, generic pseudoscalars or axion-like particles (ALPs) have been hypothesized by many extensions of the standard model of particle physics. Theories such as Supergravity [39] and Superstring theory [40] contain many broken U(1) symmetries, that can lead to very light scalar, or pseudoscalar, particles.

Pulsars, discovered fifty years back [41], are a fusion fuel less state of a two to three solar mass (M_{\odot}) star [42], wherein surmounting inward gravitational pull [43], in absence of a commensurate radiation pressure from fusion,

makes it collapse [44], into a tiny object [45]. Two effects follow: the protons and neutrons coalesce together making the Pulsars synonymous with neutron stars [46]; and, also during this compression phase the the magnetic flux is conserved, thereby promoting the magnetic induction field inside it to a colossal [46] value. Other effects such as the ‘pulsating’ nature of the ‘star’ in its last phase of stellar evolution, leading to the nomenclature & discovery of the same [46], won’t be pursued here.

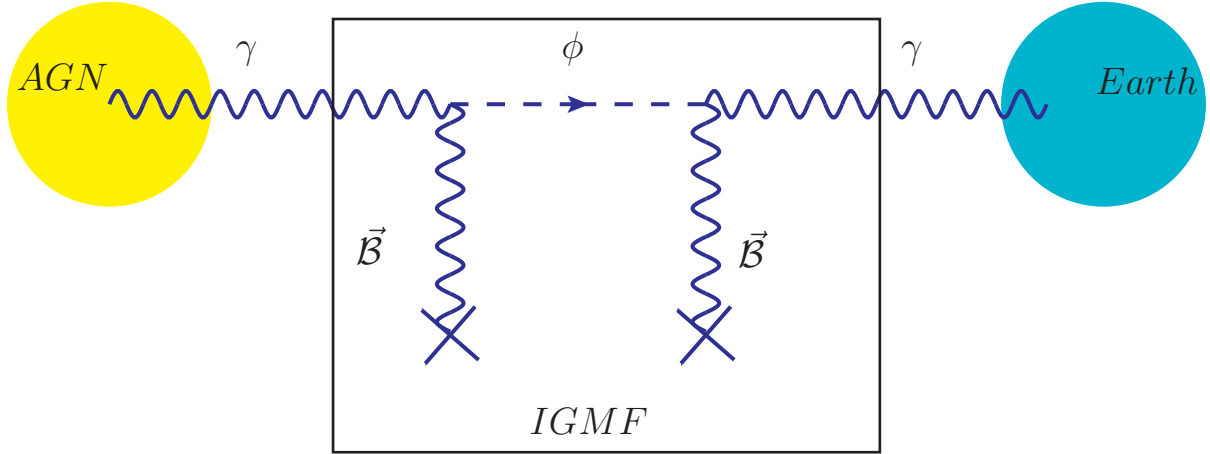


Figure 1: Axion Photon Mixing In The Interstellar Medium

Pulsars have been harnessed to estimate the coloumn density [47], by observing Pulsar dispersion measure. Also, the magnetic field of the interstellar medium (henceforth ISM) [47] along the line of sight can be estimated by observing its rotation measure [47]. Pulsars were traditionally, observed on earth inside the radio frequency window specifically, from 100MHz – 100GHz [46]. However, over time, pulsars became known for emission in other wavebands like X-ray & γ -ray, etc [48]. Despite, half a century of efforts, the mechanisms for such types of radiation and properties thereof, such as polarisation etc. are not very well understood [49]. This in turn banks heavily on the fact that pulsar atmosphere or its magnetosphere models are still in its infancy [50]. There are competing contenders as preferred models for pulsed emission and continuum radiation. Curvature radiation, synchrotron radiation, inverse Compton radiation, superconducting self Compton radiation etc. are at the forefront, but none fits all observational features of pulsars [49]. We shall, however, restrict ourselves, polarisation properties of radiation inside the pulsar atmosphere without looking into the radiation origin. Here we shall harness the two pulsar properties the size, and magnetic field which in turn is deduced from period and associated derivative, to estimate the pseudoscalar parameters like the mass and its coupling to photons, with the help of 21 cm observations.

In section no. 2 we describe the polarimetric data set on six hundred pulsars [51], along with the quantities that can be derived from these observed parameters assuming a basic pulsar model [46]. The observation of circular polarisation is hitherto unexplained by radiation models, theoretical [52–54] & statistical [55] alike, so far. Thereafter, in the section no. 3, we invoke the light quanta to pseudoscalar interaction to step wise calculate the correlators, ab initio, between the three degrees of freedom. Thereby, in section no. 4 we digress to stokes parameters; the experimental interface with theoretical quantities like ellipticity parameter and polarisation position angle, using the definition of correlators. In the next section 5, we discuss the extraction process of pseudoscalar parameters, for mixing case only, discarding another two cases and leaving the general case open that might arise, naturally. Also in this segment we estimate the values of regression parameters derived from statistical analysis of the data set tables. In the next section we present our results. Thereafter, we conclude by projecting the feasibility of our result and scope in future directions.

2 Observation

The following data shown in table no. (1) is a small part of the data obtained from the reference no. [51]. It contains the spin down luminosity \dot{E} [44] and pulsar spin period P [45] all six hundred of them. Following the basic pulsar model [46, 56] we may derive pulsar parameters such as spin period time derivative \dot{P} and the magnetic field B_s .

$$\begin{aligned} B_s &= 3.2 \times 10^{19} \times \sqrt{P\dot{P}} \\ \dot{P} &= \frac{\dot{E}P^3}{4\pi^2 I} \end{aligned} \quad (2.1)$$

Also, from the ratio between the percentage of circular to linear polarisation provides us with the ellipticity parameter χ .

$$\tan(2\chi) = \frac{V}{L} \quad (2.2)$$

We have tabulated these derived values for use and is given in Appendix.

3 Pseudoscalar Photon Mixing

The following mixing matrix (eqn. no. 3.1) provides for the necessary ingredient of photon pseudoscalar mixing mediated by a magnetic field [57]. Also this reference assumes a free space, for calculation, hence there are no Faraday effect (M_{21} & M_{12} entries) terms coupling the two photon polarisations. Inside pulsar magnetosphere this could hardly be the case. However, we may still ignore the Faraday terms. The reason being the smallness of it inside spaces with large magnetic fields; as shown in by one of the coauthors [58], by deriving the limiting propagation frequency, below which Faraday effect holds significance.

$$\omega_L = \frac{\omega_p^2 \omega_B (\omega_p^2 - m_a^2) \cos \Theta}{|B|^2 \sin^2 \Theta}$$

for the values derived from the pulsar database, such as the magnetic field, and the plasma frequency from literature [59], which is much smaller than the pseudoscalar mass, we see that Faraday effect can safely be neglected at the operating frequency of 1.4 GHz ($\gg \omega_L$), with which the observations were made.

$$M = \begin{pmatrix} A_1 & 0 & 0 \\ 0 & A_2 & T \\ 0 & T & -B \end{pmatrix}, \quad (3.1)$$

Where the symbols in the matrix [3.1] stands for

$$\begin{aligned} A_1 &= 4\omega^2 \xi \sin^2 \Theta + \omega_p^2 \\ A_2 &= 7\omega^2 \xi \sin^2 \Theta + \omega_p^2, \\ B &= m_a^2, \\ T &= gB\omega. \end{aligned} \quad (3.2)$$

where, B is the magnetic field, Θ is the angle between the \vec{k} and the magnetic field B , m_a the axion mass, and $\xi = \frac{\alpha}{4\pi} \left(\frac{eB}{m_f^2} \right)^2$, with m_f [57] the lightest Fermion mass.

The non diagonal 2×2 matrix, in eqn.3.1 is given by,

$$M_2 = \begin{pmatrix} A_2 & T \\ T & -B \end{pmatrix}. \quad (3.3)$$

One can solve for the eigen values of the eqn. [3.4], from the determinant equation,

Table 1: Pulsar polarisation properties at 1.4 GHz (sample)

Jname	Period (ms)	DM (cm^{-3}pc)	RM (radm^{-2})	$\log(\dot{E})$ (ergs^{-1})	nbin	σ_I (mJy)	$S_{1.4}$ (mJy)	W_{50} (deg)	L/I %	V/I %	$ V /I$ %	err %	flag
J0034-0721	943.0	10.9	9.8	31.3	1024	0.27	11.12	14.4	10.7	7.7	7.5	3.0	
J0051+0423	354.7	13.9	-30.5	30.8	512	0.39	0.49	26.0	13.1	-2.3	11.2	3.3	
J0108-1431	807.6	2.4	-0.3	30.8	1024	0.57	1.37	11.6	76.7	15.5	13.1	3.1	
J0134-2937	137.0	21.8	13.0	33.1	1024	0.37	3.90	4.9	45.3	-17.2	16.9	3.0	
J0151-0635	1464.7	25.7	-7.0	30.7	512	1.01	1.57	28.8	29.1	-1.7	4.2	3.3	
J0152-1637	832.7	11.9	2.0	31.9	1024	0.44	2.14	6.3	15.1	1.1	6.0	3.0	
J0206-4028	630.6	12.9	-4.0	32.3	1024	0.51	0.75	2.8	10.6	9.3	9.9	3.1	
J0211-8159	1077.3	24.4	54.0	31.0	512	0.77	0.33	16.2	17.0	11.7	15.4	5.5	W
J0255-5304	447.7	15.9	32.0	31.1	1024	0.65	5.00	6.0	7.3	-4.1	5.5	3.0	
J0304+1932	1387.6	15.7	-8.3	31.3	1024	0.92	15.05	10.9	33.4	15.1	14.8	3.0	
J0343-3000	2597.0	20.2	33.7	29.1	1024	0.96	1.26	4.9	14.3	3.1	3.9	3.2	
J0401-7608	545.3	21.6	19.0	32.6	1024	0.42	3.80	13.4	28.6	-0.1	4.7	3.0	
J0448-2749	450.4	26.2	24.0	31.8	1024	1.01	2.04	8.4	23.9	-13.3	11.8	3.0	
J0450-1248	438.0	37.0	13.0	31.7	512	1.01	1.22	20.4	25.3	2.5	6.0	3.4	
J0452-1759	548.9	39.9	13.8	33.1	1024	0.47	16.83	17.6	18.9	3.6	4.2	3.0	
J0459-0210	1133.1	21.0	18.0	31.6	1024	1.50	0.63	3.2	10.4	-12.9	9.6	3.8	
J0520-2553	241.6	33.8	19.0	31.9	512	0.96	0.79	14.1	18.2	-4.3	5.0	3.6	
J0525+1115	354.4	79.4	37.0	31.8	1024	0.58	1.74	14.1	10.6	12.5	15.5	3.0	
J0528+2200	3745.5	50.9	-40.2	31.5	2048	2.48	8.90	14.6	36.9	-4.9	4.6	3.0	
J0533+0402	963.0	83.7	-71.2	30.9	1024	0.86	0.73	5.6	13.3	4.0	5.5	3.2	
J0536-7543	1245.9	17.5	25.2	31.1	1024	0.58	8.42	16.5	48.8	-11.1	11.0	3.0	
J0540-7125	1286.0	29.4	43.0	31.2	512	0.94	0.35	8.4	14.2	3.1	15.8	4.8	
J0543+2329	246.0	77.7	8.7	34.6	1024	0.53	12.90	7.7	45.2	-8.2	7.9	3.0	
J0601-0527	396.0	80.5	64.0	32.9	1024	0.62	2.59	14.4	30.9	4.4	11.3	3.0	
J0614+2229	335.0	96.9	69.0	34.8	1024	0.73	3.60	6.7	72.0	20.3	20.1	3.0	

$$\begin{vmatrix} A_2 - \lambda & T \\ T & -B - \lambda \end{vmatrix} = 0, \quad (3.4)$$

and the roots are,

$$M_{\pm} = \frac{A_2 - B}{2} \pm \frac{1}{2} \sqrt{[(A_2 + B)^2 + 4T^2]}. \quad (3.5)$$

$$(3.6)$$

3.1 Equation of Motion

The equation of motion for the axion photon mixing, in the non diagonal basis gets decoupled and can be written in the matrix form as,

$$[(\omega^2 + \partial_z^2) \mathbf{I} + \mathbf{M}] \begin{pmatrix} A_{\perp} \\ A_{\parallel} \\ a \end{pmatrix} = 0. \quad (3.7)$$

where \mathbf{I} is a 3×3 identity matrix and \mathbf{M} is the mixing matrix.

The uncoupled and the coupled equations can further be written as,

$$[(\omega^2 + \partial_z^2) + A_1] (A_{\perp}) = 0. \quad (3.8)$$

and

$$[(\omega^2 + \partial_z^2) \mathbf{I} + M_2] \begin{pmatrix} A_{\parallel} \\ a \end{pmatrix} = 0. \quad (3.9)$$

It is possible to diagonalise eqn.[3.9] by a similarity transformation (we would denote the diagonalising matrix by O), leading to the form,

$$[(\omega^2 + \partial_z^2) \mathbf{I} + M_D] \begin{pmatrix} \bar{A}_{\parallel} \\ \bar{a} \end{pmatrix} = 0. \quad (3.10)$$

when the diagonal matrix M_D is given by:

$$M_D = \begin{pmatrix} M_+ & 0 \\ 0 & M_- \end{pmatrix} \quad (3.11)$$

3.2 Dispersion Relations

Defining the wave vectors in terms of k_i 's, as:

$$\begin{aligned} k_{\perp} &= \sqrt{\omega^2 + A_1} \\ k_+ &= \sqrt{\omega^2 + M_+} \\ k_- &= -\sqrt{\omega^2 + M_+} \end{aligned} \quad (3.12)$$

and

$$\begin{aligned} k'_+ &= \sqrt{\omega^2 + M_-} \\ k'_- &= -\sqrt{\omega^2 + M_-} \end{aligned} \quad (3.13)$$

3.3 Solutions

The solutions for the gauge field and the axion field, given by [3.10] as well as the solution for eqn. for A_{\perp} in k space can be written as,

$$\bar{A}_{\parallel}(z) = \bar{A}_{\parallel+}(0)e^{ik_+z} + \bar{A}_{\parallel-}(0)e^{-ik_-z} \quad (3.14)$$

$$\bar{a}(z) = \bar{a}_+(0)e^{ik'_+z} + \bar{a}_-(0)e^{-ik'_-z} \quad (3.15)$$

$$A_{\perp}(z) = A_{\perp+}(0)e^{ik_{\perp}z} + A_{\perp-}(0)e^{-ik_{\perp}z} \quad (3.16)$$

$$(3.17)$$

The diagonal matrix can be written as

$$M_D = O^T M_2 O \quad (3.18)$$

when

$$O = \begin{pmatrix} \cos \theta & -\sin \theta \\ \sin \theta & \cos \theta \end{pmatrix} \equiv \begin{pmatrix} c & -s \\ s & c \end{pmatrix}. \quad (3.19)$$

in short hand notation.

3.4 Similarity Transformation

The diagonal matrix

$$M_D = \begin{pmatrix} c & s \\ -s & c \end{pmatrix} \begin{pmatrix} M_{11} & M_{12} \\ M_{21} & M_{22} \end{pmatrix} \begin{pmatrix} c & -s \\ s & c \end{pmatrix}, \quad (3.20)$$

With $M_{11} = A_2$, $M_{12} = T$, $M_{21} = T$ lastly $M_{22} = -B$.

The value of the parameter θ , is fixed from the equality,

$$M_D = \begin{pmatrix} c & s \\ -s & c \end{pmatrix} \begin{pmatrix} M_{11} & M_{12} \\ M_{21} & M_{22} \end{pmatrix} \begin{pmatrix} c & -s \\ s & c \end{pmatrix} = \begin{pmatrix} M_+ & 0 \\ 0 & M_- \end{pmatrix}, \quad (3.21)$$

leading to,

$$\begin{pmatrix} c^2 M_{11} + s^2 M_{22} + 2cs M_{12} & M_{12}(c^2 - s^2) + cs(M_{22} - M_{11}) \\ M_{12}(c^2 - s^2) + cs(M_{22} - M_{11}) & s^2 M_{11} + c^2 M_{22} - 2cs M_{12} \end{pmatrix} = \begin{pmatrix} M_+ & 0 \\ 0 & M_- \end{pmatrix}, \quad (3.22)$$

Equating the components of the matrix equation [3.22], one arrives at:

$$\tan(2\theta) = \frac{2M_{12}}{M_{11} - M_{22}} = \frac{2T}{A_2 + m_a^2}. \quad (3.23)$$

3.5 Correlation Functions

The solutions for propagation along the +ve z axis, is given by,

$$\bar{A}_{\parallel}(z) = \bar{A}_{\parallel+}(0)e^{ik_+z} \quad (3.24)$$

$$\bar{a}(z) = \bar{a}_+(0)e^{ik'_+z} \quad (3.25)$$

$$(3.26)$$

that can further be written in the following form,

$$\begin{pmatrix} \bar{A}_{||}(z) \\ \bar{a}(z) \end{pmatrix} = \begin{pmatrix} e^{ik_+z} & 0 \\ 0 & e^{ik'_+z} \end{pmatrix} \begin{pmatrix} \bar{A}_{||}(0) \\ \bar{a}(0) \end{pmatrix}. \quad (3.27)$$

Since,

$$\begin{pmatrix} \bar{A}_{||}(z/0) \\ \bar{a}(z/0) \end{pmatrix} = O^T \begin{pmatrix} A_{||}(z/0) \\ a(z/0) \end{pmatrix}. \quad (3.28)$$

it follows from there that,

$$\begin{pmatrix} A_{||}(z) \\ a(z) \end{pmatrix} = O \begin{pmatrix} e^{ik_+z} & 0 \\ 0 & e^{ik'_+z} \end{pmatrix} O^T \begin{pmatrix} A_{||}(0) \\ a(0) \end{pmatrix}. \quad (3.29)$$

Using eqn.[3.29] we arrive at the relation,

$$A_{||}(z) = \left[e^{ik_+z} \cos^2\theta + e^{ik'_+z} \sin^2\theta \right] A_{||}(0) + \left[e^{ik_+z} - e^{ik'_+z} \right] \cos\theta \sin\theta a(0) \quad (3.30)$$

$$a(z) = \left[e^{ik_+z} - e^{ik'_+z} \right] \cos\theta \sin\theta A_{||}(0) + \left[e^{ik_+z} \sin^2\theta + e^{ik'_+z} \cos^2\theta \right] a(0) \quad (3.31)$$

If the axion field is zero to begin with, i.e

$$a(0) = 0. \quad (3.32)$$

Then the solution for the gauge fields take the following form,

$$A_{||}(z) = \left[e^{ik_+z} \cos^2\theta + e^{ik'_+z} \sin^2\theta \right] A_{||}(0) \quad (3.33)$$

$$A_{\perp}(z) = e^{ik_{\perp}z} A_{\perp}(0). \quad (3.34)$$

The correlations of different components take the following form:

$$\langle A_{||}^*(z) A_{||}(z) \rangle = \left[\cos^4\theta + \sin^4\theta + 2 \sin^2\theta \cos^2\theta \cos[(k_+ - k'_+)z] \right] \langle A_{||}^*(0) A_{||}(0) \rangle \quad (3.35)$$

$$\langle A_{||}^*(z) A_{\perp}(z) \rangle = \left[\cos^2\theta e^{i(k_{\perp} - k_+)z} + \sin^2\theta e^{i(k_{\perp} - k'_+)z} \right] \langle A_{||}^*(0) A_{\perp}(0) \rangle \quad (3.36)$$

$$\langle A_{\perp}^*(z) A_{\perp}(z) \rangle = \langle A_{\perp}^*(0) A_{\perp}(0) \rangle \quad (3.37)$$

4 Stokes Parameters

Using the definitions of the Stokes parameters, in terms of the correlators:

$$I = \langle A_{||}^*(z) A_{||}(z) \rangle + \langle A_{\perp}^*(z) A_{\perp}(z) \rangle, \quad (4.1)$$

$$Q = \langle A_{||}^*(z) A_{||}(z) \rangle - \langle A_{\perp}^*(z) A_{\perp}(z) \rangle, \quad (4.2)$$

$$U = 2\text{Re} \langle A_{||}^*(z) A_{\perp}(z) \rangle, \quad (4.3)$$

$$V = 2\text{Im} \langle A_{||}^*(z) A_{\perp}(z) \rangle. \quad (4.4)$$

Using the relations for the corresponding correlators, the stokes parameters turn out to be

$$\begin{aligned}
I &= [\cos^4\theta + \sin^4\theta + 2\sin^2\theta \cos^2\theta \cos[(k_+ - k'_+)z]] \langle A_{||}^*(0)A_{||}(0) \rangle + \langle A_{\perp}^*(0)A_{\perp}(0) \rangle \\
Q &= [\cos^4\theta + \sin^4\theta + 2\sin^2\theta \cos^2\theta \cos[(k_+ - k'_+)z]] \langle A_{||}^*(0)A_{||}(0) \rangle - \langle A_{\perp}^*(0)A_{\perp}(0) \rangle \\
U &= 2([\cos^2\theta \cos[(k_{\perp} - k_+)z]] + \sin^2\theta \cos[(k_{\perp} - k'_+)z]) \langle A_{||}^*(0)A_{\perp}(0) \rangle \\
V &= 2([\cos^2\theta \sin[(k_{\perp} - k_+)z]] + \sin^2\theta \sin[(k_{\perp} - k'_+)z]) \langle A_{||}^*(0)A_{\perp}(0) \rangle
\end{aligned} \tag{4.5}$$

The Stokes parameters are also expressed as such

$$I = I_p \tag{4.6}$$

$$Q = I_p \cos 2\psi \cos 2\chi \tag{4.7}$$

$$U = I_p \sin 2\psi \cos 2\chi \tag{4.8}$$

$$V = I_p \sin 2\chi. \tag{4.9}$$

where χ & ψ are usual ellipticity parameter and the polarisation position angle. The degree of (linear /) polarisation is given by,

$$\begin{aligned}
p &= \frac{\sqrt{Q^2 + U^2 + V^2}}{I_p} \\
p_{lin} &= \frac{\sqrt{Q^2 + U^2}}{I_p}
\end{aligned} \tag{4.10}$$

and the linear polarisation angle is given by

$$\begin{aligned}
\tan 2\psi &= \frac{U}{Q} \\
\tan 2\chi &= \frac{V}{p_{lin}}
\end{aligned} \tag{4.11}$$

It has been noted in [60], that in case, we make any coordinate transformation around the axis of photon propagation the two linear polarisation become mixed. Hence, we need to be careful, as our solution process entails a similarity transformation. To see this we define the density matrix

$$\rho(z) = \begin{pmatrix} \langle A_{||}^*(z)A_{||}(z) \rangle & \langle A_{||}(z)A_{\perp}^*(z) \rangle \\ \langle A_{||}^*(z)A_{\perp}(z) \rangle & \langle A_{\perp}^*(z)A_{\perp}(z) \rangle \end{pmatrix} = \frac{1}{2} \begin{pmatrix} I(z) + Q(z) & U(z) - iV(z) \\ U(z) + iV(z) & I(z) - Q(z) \end{pmatrix} \tag{4.12}$$

if we rotate the density matrix by an amount α about an axis perpendicular the plane containing $A_{||}(z)$ & $A_{\perp}(z)$, the density matrix transforms as $\rho(z) \rightarrow \rho'(z)$ given such to be

$$\rho'(z) = \frac{1}{2} R(\alpha) \begin{pmatrix} I(z) + Q(z) & U(z) - iV(z) \\ U(z) + iV(z) & I(z) - Q(z) \end{pmatrix} R^{-1}(\alpha) \tag{4.13}$$

where,

$$R(\alpha) = \begin{pmatrix} \cos \alpha & -\sin \alpha \\ \sin \alpha & \cos \alpha \end{pmatrix} \tag{4.14}$$

Under such transformation the $I(z)$ & $V(z)$ remains unaltered. However, the $Q(z)$ & $U(z)$ starts mixing with each other by the following

$$\begin{pmatrix} Q'(z) \\ U'(z) \end{pmatrix} = \begin{pmatrix} \cos 2\alpha & \sin 2\alpha \\ -\sin 2\alpha & \cos 2\alpha \end{pmatrix} \begin{pmatrix} Q(z) \\ U(z) \end{pmatrix} \tag{4.15}$$

We conclude this section by mentioning that in such a case the ellipticity parameter remains unaltered but the polarisation position angle changes by 2α as given below

$$\begin{aligned}
\tan(2\chi') &= \tan(2\chi) \\
\tan(2\psi') &= \tan(2\alpha + 2\psi)
\end{aligned} \tag{4.16}$$

5 Ellipticity Parameter & Polarization Position Angle

As a follow-up to the analytical expressions given in the previous section/s, we consider two special case of the stokes parameter where either one of the two effects, namely, the mixing effect or, the Cotton-Mouton effect would be absent. Thereafter we shall consider the general formula. In each case, we would like to obtain the value of the ellipticity angle χ after propagation a fixed distance z of light and determine it's frequency dependence. For all the three cases we shall assume the light to be completely plane polarised in the transverse direction, or U polarised. This is common observance in Pulsar polarisation cases.

5.1 Case - I: Mixing Only

Here we assume that the Cotton Mouton term (i.e. ξ term inside the diagonal ones A_1, A_2) are absent. We also assume a pseudoscalar mass which is much less than the plasma frequency here. This greatly simplifies calculation without being much deviant from the reality, if we consider the parameters of the pulsar environment. Next we consider how the circular polarisation varies in this case. Assuming $\theta \ll 1$ one have

$$V = \left(\sin [(k_{\perp} - k_{+}) z] + \left[\frac{g\mathfrak{B}\omega}{\omega_p^2 + m_a^2} \right]^2 \sin [(k_{\perp} - k'_{+}) z] \right) \langle A_{\parallel}^*(0) A_{\perp}(0) \rangle \quad (5.1)$$

Following the set of eqns. 3.12-3.13 we can simplify the arguments of the remaining sinusoids of eqn. no. 5.1 as given below :

$$k_{\perp} - k_{+} = - \left\{ \frac{(g\mathfrak{B}\omega)^2}{2(\omega_p^2 + m_a^2)\omega} \right\} \quad k_{\perp} - k'_{+} = + \left\{ \frac{(g\mathfrak{B}\omega)^2}{2(\omega_p^2 + m_a^2)\omega} + \frac{m_a^2}{2\omega} \right\} \quad (5.2)$$

So, if $\xi = 0$, then the ellipticity parameter to its lowest order ($\propto \theta^2$) is found to be as follows, which matches well with [60,61], though the later most probably has a typo ⁽¹⁾.

$$\chi \approx \frac{1}{96\omega} (g\mathfrak{B}m_a)^2 z^3 \quad (5.3)$$

Similarly, we may now turn our attention to two linear polarisation degrees of freedom, where the mixing angle $\theta \ll 1$, is small, to figure out the polarisation position angle.

$$\tan(2\psi) = \frac{U}{Q} \quad (5.4)$$

However, in the beginning of this section we have already mentioned that $U \simeq 1$. This is true for the parameters of interest used here and the observational cases to be discussed later. This makes the polarisation position angle inversely proportional to Q . But before we evaluate the expression for Q , we note that in the case of mixing the beam is assumed to propagate at an angle $\frac{\pi}{4}$ as compared to the magnetic field of the Pulsar. Hence we need to change our expression for polarisation position angle accordingly. As discussed during derivation of eqn. no. (4.16), we have;

$$\tan \left(2\psi + \frac{\pi}{2} \right) = \frac{1}{Q} \quad (5.5)$$

Next, we evaluate Q keeping in mind the approximations made before. Keeping terms up to order θ^2 in the expression for Q , we have,

$$Q = -2\theta^2 \left[\sin^2 \left(\frac{\langle k_{+} - k'_{+} \rangle z}{2} \right) \right] \quad (5.6)$$

Again, following the set of Eqns. 3.12-3.13, we have

$$\langle k_{+} - k'_{+} \rangle \simeq \frac{m_a^2}{2\omega} \quad (5.7)$$

⁽¹⁾It claimed concurrence with the former but is actually at variance, with it

Linear Regression for Coupling

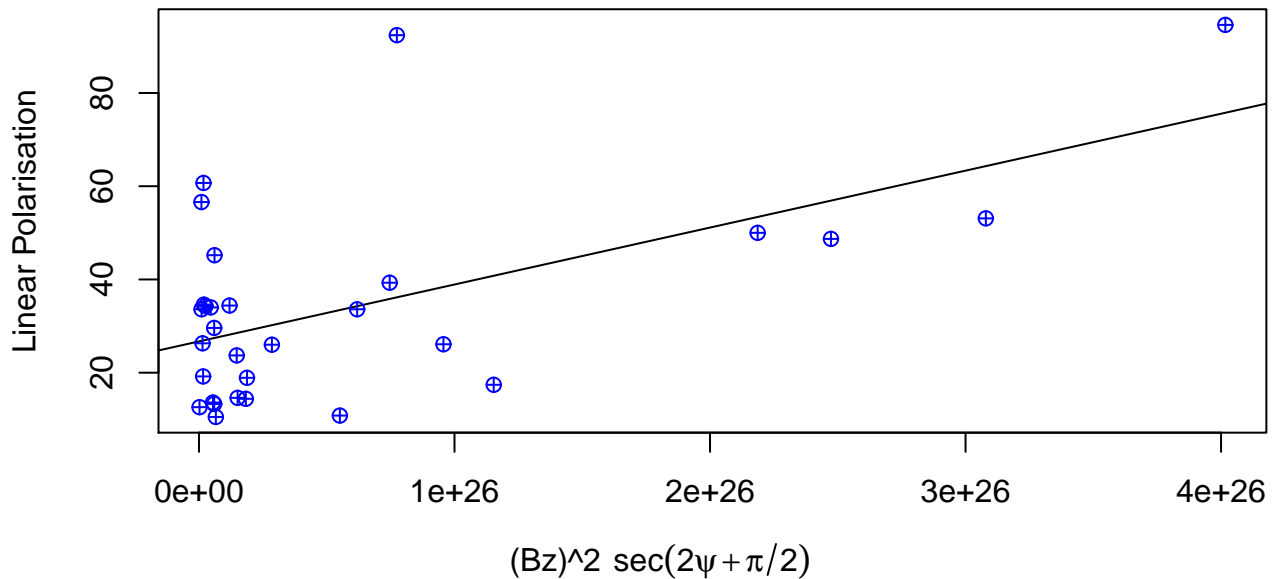


Figure 2: Linear regression between PPAs and Lin. Pol.

Substituting, one gets, in conjunction with [61]

$$\psi = \frac{1}{16} (g\mathfrak{B}z)^2 \quad (5.8)$$

However, unlike the circular polarisation, which was attributed to its entirety, to the mixing effect, one can not ascribe the entire pulsar linear polarisation [62] to this tiny mixing effect, where the mixing angle $\theta \ll 1$. So, we note that the pulsar radio emission is inherently linearly polarised to a large degree, due to curvature, synchrotron and superconducting self Compton effects thereof. We use $U \simeq 1$ and only the Q part is modelled vis-a-vis pseudoscalar photon mixing; where

$$Q = \frac{1}{8} (g\mathfrak{B}z)^2 \quad (5.9)$$

along with the definitive couple of eqn. (4.11) to note that the linear polarisation observed is equal to

$$p_{lin} = Q \sec\left(2\psi + \frac{\pi}{2}\right) \quad (5.10)$$

We note that the determination process of absolute pulsar polarisation [63, absolute PPAs] position angles, is now experimentally feasible and the same values have already been scraped out for 30 (thirty) odd pulsars. The literature contains a little less than fifty absolute PPAs from [64, absolute polarisation position angles for 47 odd pulsars], out of which only 30 (thirty) cross matched with that of our old set of 537 data, used to calculate the ellipticity parameter. The expression for Q has only one unknown, the coupling of pseudoscalar with photons. Hence, we may do a regression analysis here, too, to estimate the same. The summary table is given in table no. (2).

For the sake of brevity, we post a small segment of total 47 pulsar given in reference [64] in table no. (3). The pulsar names here are catalogued in B1950 almanac standard, which were then converted to J2000 almanac standard and cross matched with the original & usable 537 strong population data on pulsar polarisation. Thirty (30) odd samples of them were found to be common in both.

Coefficients	Mean	Std.-Error	F-statistics	t-value	Pr(> t)
Slope	2.404e-25	4.567e-26	27.7196	5.265	1.21e-05

Table 2: Regression Result for the coupling of the pseudoscalar

Table 3: Small Sample of Absolute Pulsar Polarisation Position Angles, from [64].

Pulsar	PA_V (deg)	PA_0	Ψ (deg)
B0011+47	+136(3)	43(7)	-87(8)
B0136+57	-131(0)	43(3)	6(3)
B0329+54	119(1)	20(4)	99(4)
B0355+54	48(1)	-41(4)	89(5)
B0450+55	108(0)	-23(16)	-94(16)
B0450-18	40(5)	47(3)	-7(6)
B0540+23	58(19)	-85(3)	-37(19)
B0628-28	294(2)	26(2)	88(3)
B0736-40	227(5)	-44(5)	91(7)

Linear Regression for Mass

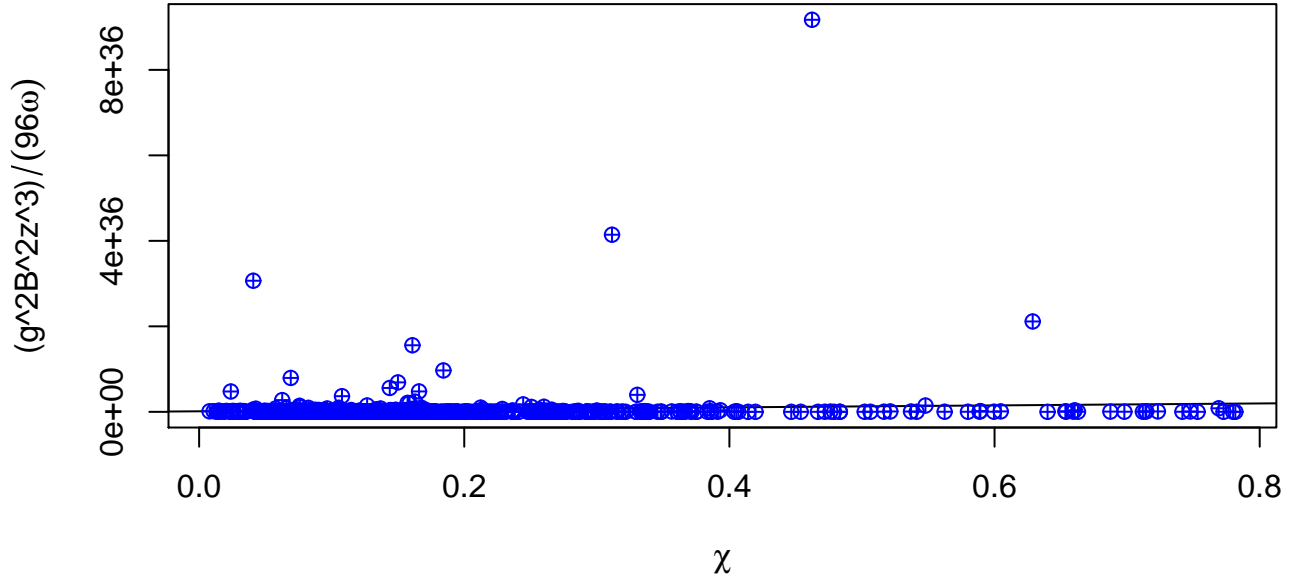


Figure 3: Linear regression between observed & (scaled) theoretical ellipticity parameter

Now, we turn our attention back to the ellipticity parameter given in equation no. (5.3). Being a small angle, we have relegated the tangent as equivalent to its angular argument. The regression analysis thus to be undertaken is between circular and linear random variables, lying on LHS (ellipticity parameter) and RHS (magnetic field) respectively. Suffice it to say that the LHS is readily read off from the table no. (1). The result of correlation study is given in the

Coefficients	Mean	Std.-Error	F-statistics	t-value	Pr(> t)
Slope	7.471e-38	2.251e-38	11.0164	3.319	0.000964

Table 4: Regression Result for the mass of the pseudoscalar

table no. (4)

5.2 Case - II: Cotton-Mouton Only

Here if we assume the mixing to be absent then we get $\theta = 0$ and hence we get the circular polarisation as

$$V=2 (\sin [(k_{\perp} - k_{+}) z]) < A_{\parallel}^*(0)A_{\perp}(0) > \quad (5.11)$$

Here, we need to evaluate only one argument and it is the same as given above:

$$k_{\perp} - k_{+} = \frac{1}{2\omega} \{-3\xi\} \quad (5.12)$$

We note, that, the mass of the pseudoscalar cancels and the mixing term is assumed zero. We see, that, the circular polarisation has now become inversely proportional to frequency assuming the argument to be considerably small as in the other case. Given that no circular polarisation would be produced in this case, it would be uninteresting to ponder over here.

5.3 Case III: Limiting Case

We note the essential non-linearity resulting from the two effect taken in conjunction. Since we can not just add the two effects separately, even if they both are small and perturbative, to obtain the final result. We also note that the two effects shall be competing with each other when the following condition is met

$$\omega\xi \approx gB$$

Leaving aside the numerical prefactors -tentatively we see that, unless the value of magnetic field is very large (magnetars) and the beam frequency used in experiment is quite high (unlike this case), even the modest values coming from astronomical bounds on pseudoscalar may not be comparable with the Cotton-Mouton effect & are in fact larger in effect.

5.4 Case IV: General Case

Here in this subsection we calculate the amount of circular polarisation, vide the stokes parameter V , without resorting to any of the approximations made in the preceding two subsections, for completeness. Here the expression for the V becomes

$$V=\left\{ \cos^2 \left[\frac{g\mathfrak{B}\omega}{7\xi\omega^2 \sin^2 \alpha + \omega_p^2 + m_a^2} \right] \sin [(k_{\perp} - k_{+}) z] + \sin^2 \left[\frac{g\mathfrak{B}\omega}{7\xi\omega^2 \sin^2 \alpha + \omega_p^2 + m_a^2} \right] \sin \left[(k_{\perp} - k'_{+}) z \right] \right\} < A_{\parallel}^*(0)A_{\perp}(0) > \quad (5.13)$$

Hence at lowest order the first term, in ($\theta \ll 1$) limit, would not change anything from what the first term, for the case of the pure mixing effect, did. But the second term, even at the lowest order shall render the expression for V qualitatively different from what is was then at pure mixing effect. Needless to say that pure Cotton-Mouton effect does not match, even qualitatively, with any of them, either. For completeness, we write down the values of the wave vectors again.

$$k_{\perp} - k_{+} = \frac{1}{2\omega} \left\{ \xi (4 \cos^2 \alpha - 7 \sin^2 \alpha) + \left[\frac{(g\mathfrak{B}\omega)^2}{7\xi\omega^2 \sin^2 \alpha + m_a^2} \right] \right\} \quad k_{\perp} - k'_{+} = \frac{1}{2\omega} \left\{ 4\xi \cos^2 \alpha + m_a^2 - \left[\frac{(g\mathfrak{B}\omega)^2}{7\xi\omega^2 \sin^2 \alpha + m_a^2} \right] \right\} \quad (5.14)$$

Thus far we have only shown the difference of results of all three separate cases in terms of the V parameters depicting circular polarisation. This can be done with other two linear polarisation degrees of freedom, too. We leave this for a future endeavour.

6 Result

By the careful analysis of [51, containing 600 Pulsar polarisation data, of which 537 are used here] and that of [64, containing 47 absolute PPAs for pulsars, 30 of which are common to the above], we came to the following result given in table no. (5). We however note that more data samples on absolute PPAs are required to obtain a more statistically

Results Obtained		
Parameters	Values	Significance Level
$g_{\phi\gamma\gamma}$	$4.903 \times 10^{-13} \text{ GeV}^{-1}$	$\simeq 0.001\%$
$m_{\mathbf{a}}$	$2.733 \times 10^{-10} \text{ eV}$	$< 0.1\%$

Table 5: The result of this analysis

significant result on the coupling, which is deduced, from this parameter. Currently a little over fifty (50) pulsars are amenable to this type of absolute PPA studies. The second quantity, namely the mass, has the numbers (> 500) on its side. Nonetheless, its extraction from the ellipticity parameter, in turn, hinges on the coupling value, indirectly affecting the confidence interval found from the population. Also, for the sake of thoroughness we mention that the degree of linear polarisation is claimed to be dependent on frequencies in which they are observed [65]. The PPAs that are quoted in [64, Absolute PPAs for 47 pulsars], are for various radio frequencies, e.g. 327 MHz, 691 MHz, 3.1 GHz etc., including that of 1.4 GHz, which corresponds to 21 cm. Since, there has been no connection to PPAs are made with frequency, to our knowledge to this date, we did not investigate this further.

7 Discussion & Outlook

Taking advantage of new age of data explosion arising out from newer observational techniques and that of machine tools, we tried to estimate pseudoscalar particle mass and its coupling to photons. The results thus obtained do not match any standard axion models such as DFSZ or KSVZ etc. Hence these finding must be accommodated in the fold of axion like particles (ALPs) outside of the QCD realm. Surprisingly, our bottom up study, has automatically, led us to values, that are comparable and between the contemporary theories on cosmic axion background radiation (CAB), leading to soft X-ray excesses observed from comma cluster [66] & that of the extra-galactic background light (EBL) to ALPs conversion & oscillation, leading to an observed anomalous γ ray transparency of the universe [67]. Fortunately, the previous constraints set on the mass and coupling of pseudoscalars, either by the changes in of quasar polarisation, hypothetically by ALPs [68], or by the γ ray burst SN1987A [69], occurring through a so called ALPs burst, are not in conflict with our results, either.

As mentioned in section no. (5) a future incorporation of Cotton Mouton effect into this study, may be performed, so as to see how the result on these estimates may change, for better or worse. These parameters may also be harnessed for devising CDM/WDM models and to obtain their relic densities.

Acknowledgement

The authors acknowledge the software R [70] for easing out the statistical analysis. SM is thankful of the help of K. Bhattacharya regarding the same.

References

- [1] L. Maiani; S. Petrosino & E. Zavattini. *Phys. Lett. B*, 175:359, 1986.
- [2] R. D. Peccei and H. Quinn. *Phys. Rev. Lett.*, 38:1440, 1977.
- [3] F. Wilczek. *Phys. Rev. Lett.*, 40:279, 1978.
- [4] S. Weinberg. *Phys. Rev. Lett.*, 40:223, 1978.
- [5] J. E. Kim. *Phys. Rev. Lett.*, 43:103, 1979.
- [6] L. Abbott and P. Sikivie. *Phys. Lett. B*, 120:133, 1983.
- [7] S. Das et. al. *Jour. Cosmol. Astropart Phys.*, 06(002), 2005.
- [8] Jain P.; Narain G. & Sarala S. *MNRAS*, 347:394, 2004.
- [9] Nishant Agarwal; Archana Kamal & Pankaj Jain. *Phys. Rev. D*, 83:065014, 2011.
- [10] Nishant Agarwal; Pavan K. Aluri; Pankaj Jain; Udit Khanna & Prabhakar Tiwari. *The European Physical Journal C*, 72:1928, 2012.
- [11] Prabhakar Tiwari & Pankaj Jain. *International Journal of Modern Physics D*, 22:50089, 2013.
- [12] Prabhakar Tiwari. *Phys. Rev. D*, 86:115025, 2012.
- [13] Pankaj Jain & Prabhakar Tiwari. *Mon. Not. R. Astron. Soc.*, 460(3):26982705, 2016.
- [14] S. Das et. al. *Pramana*, 70:439, 2008.
- [15] A. Payez. *Phys. Rev.*, 85:087701, 2012.
- [16] A. Payez; J.R. Cudell & D. Hutsemekers. *Phys.Rev. D*, 84:085029, 2011.
- [17] G. Raffelt H. Vogel A. Kartavtsev. *JCAP01(2017)024*, 01:024, 2017.
- [18] Vincent Pelgrims & Damien Hutsemekers. arxiv:1503.03482.
- [19] Vincent Pelgrims & Damien Hutsemekers. arxiv:1604.03937.
- [20] A. Payez. Patras Workshop on Axions, WIMPs and WISPs. In *arXiv:1309.6114*, 2013.
- [21] Alexandre Payez; Carmelo Evoli; Tobias Fischer; Maurizio Giannotti; Alessandro Mirizzi; Andreas Ringwald. *Jour. Cosmol. Astropart Phys.*, 1502(006), 2014.
- [22] D. Hutsemekers & H. Lamy. arXiv:astro-ph/0012182, December 2000.
- [23] Hutsemekers D. *Astronomy & Astrophysics*, 332:410, 1998.
- [24] Hutsemekers D.; Lamy H. *Astronomy & Astrophysics*, 367:381, 2001.
- [25] D. Hutsemekers; R. Cabanac; H. Lamy; D. Sluse. *Astron.Astrophys.*, 441:915, 2005.
- [26] Damien Hutsemekers; Lorraine Braibant; Vincent Pelgrims and Dominique Sluse. *Astron. Astrophys.*, 572(A18), 2014.
- [27] D. Hutsemekers; B. Borguet; D. Sluse; R. Cabanac and H. Lamy. *Astron. Astrophys.*, 520(L7), 2010.
- [28] N. Jackson; R. A. Battye; I. W. A. Browne; S. Joshi; T. W. B. Muxlow and P. N. Wilkinson. *Mon. Not. R. Astron. Soc.*, 376:371377, 2007.

- [29] A. R.; Jagannathan P. Taylor. *Mon. Not. R. Astron. Soc.*, 459(1):L36L40, 2016.
- [30] C. Csaki et. al. *Jour. Cosmol. Astropart Phys.*, 0305(005), 2003.
- [31] D. Hutsemekers; J.R. Cudell & A. Payez. Invisible Universe International Conference. In *AIP Conf. Proc.*, volume 1038, page 211, 2008. arXiv:0805.3946.
- [32] R. D. Peccei & H. Quinn. *Phys. Rev. D*, 16:1791, 1977.
- [33] A. Pich. arXiv:hep-ph/9505231v1, May 1995.
- [34] M. Dine. arXiv:hep-ph/0011376v2, November 2000.
- [35] P. Sikivie. *Phys. Rev. D*, 32:2988, 1985.
- [36] E. Kolb & M. S. Turner. *The Early Universe*. Westview Press, 2nd ed. edition, 1994. Chap 10.
- [37] W. Fischler & M. Srednicki M. Dine. *Phys. Lett. B*, 104:199, 1981.
- [38] M. A. Shifman; A. I. Vainshtein & V. I. Zakharov. *Nucl. Phys. B*, 166:493, 1980.
- [39] P. Majumdar & S. Sengupta. *Class. Quant. Grav.*, 16:L89, 1999.
- [40] A. Sen. *Int. Jour. Mod. Phys. A*, 16:4011, 2001.
- [41] A. Hewish; S. J. Bell; J. D. H. Pilkington; P. F. Scott; & R. A. Collins. Observation of a Rapidly Pulsating Radio Source. *Nature*, 217:709, 1968.
- [42] M. S. Longair. *High energy astrophysics*, volume 2. Cambridge University Press, 1994. p.99.
- [43] M. S. Longair. *Our evolving universe*. CUP Archive, 1996. p.72.
- [44] Pulsar Properties. Webpage - <https://www.cv.nrao.edu/course/astr534/PDFnewfiles/Pulsars.pdf>.
- [45] Anne Lohfink. Pulsars. webpage - <https://www.astro.umd.edu/~alohfink/seminar.pdf>, November 2008.
- [46] Duncan Ross Lorimar and Michael Kramer. *Handbook of Pulsar Astronomy*. Cambridge University Press, 2005.
- [47] W. M. Yan et. al. Polarization observations of 20 millisecond pulsars. *Mon. Not. R. Astron. Soc.*, 414:20872100, 2011.
- [48] Alice K. Harding and Constantinos Kalapotharakos. Multiwavelength Polarization of Rotation-Powered Pulsars. 2017. arXiv:1704.06183.
- [49] *New Advances in Pulsar Magnetosphere Modelling*, PoS. SISSA, 2017. arXiv:1702.00732.
- [50] Vasily Beskin. Pulsar Magnetospheres and Pulsar Winds, 2016. arXiv:1610.03365.
- [51] Simon Johnston and Matthew Kerr. Polarimetry of 600 pulsars from observations at 1.4 GHz with the Parkes radio telescope. *Mon. Not. R. Astron. Soc.*, 474(4):46294636, March 2018.
- [52] P. F. Wang, C. Wang, and J. L. Han. Curvature radiation in rotating pulsar magnetosphere. *Mon. Not. R. Astron. Soc.*, 423(1):24642475, 2012.
- [53] R. T. Gangadhara. *The Astrophysical Journal*, 710:2944, 2010.
- [54] Houshang Ardavan, Arzhang Ardavan, Joseph Fasel, John Middleditch, Mario Perez, Andrea Schmidt, and John Singleton. A new mechanism for generating broadband pulsar-like polarization. Number 78, page 16. Sissa, 2008.

- [55] Mark M. McKinnon. Statistical modeling of the circular polarization in pulsar radio emission and detection statistics of radio polarimetry. 568:302–311, 2002.
- [56] Phrudth Jaroenjittichai. *Pulsar Polarization As A Diagnostic Tool*. PhD thesis, Physics & Astronomy(UoM), 2013.
- [57] Georg Raffelt and Leo Stodolsky. Mixing of the photon with low-mass particles. *Phys. Rev. D*, 376(5), Mar 1988.
- [58] Avijit K. Ganguly; Pankaj Jain & Subhayan Mandal. *Phys.Rev.D*, 79:115014, 2009.
- [59] D.B. Melrose and M. Z. Rafat. Pulsar radio emission mechanism: Why no consensus? *J. Phys.: Conf. Ser.*, 932:012011, 2017. doi :10.1088/1742-6596/932/1/012011.
- [60] Avijit K. Ganguly. Introduction to Axion Photon Interaction in Particle Physics and Photon Dispersion in Magnetized Media. In Eugene Kennedy, editor, *Particle Physics*, chapter 3, page 4974. InTech, April 2012.
- [61] R. Cameron et al. Search for nearly massless, weakly coupled particles by optical systems. *Phys. Rev. D*, 47(9):37073725, 1999.
- [62] M. Gedalin, E. Gruman, and D. B. Melrose. *Phys. Rev. Lett.*, 88:121101, 2002.
- [63] Megan M. Force Paul Demorest Joanna M. Rankin. Absolute Polarization Determinations of 33 Pulsars Using the Green Bank Telescope. *Monthly Notices of the Royal Astronomical Society*, (4):44854499.
- [64] Joanna M. Rankin. *The Astrophysical Journal*, 804:112, 2015.
- [65] P. F. Wang, C. Wang, and J. L. Han. On the frequency dependence of pulsar linear polarization. *Mon. Not. R. Astron. Society*, 448(1):771–780, 2015.
- [66] J. P. Conlon and M. C. D. Marsh. *Phys. Rev. Lett.*, 111(15):151301, 2013.
- [67] M. Meyer, D. Horns, and M. Raue. *Phys. Rev. D*, 87:035027, 2013.
- [68] A. Payez; J.R. Cudell & D. Hutsemekers. *Jour. Cosmol. Astropart Phys.*, 1207(041), 2012.
- [69] A. Payez, C. Evoli, T. Fischer, M. Giannotti, and A. Mirizzi. Revisiting the SN1987A gamma-ray limit on ultralight axion-like particles. *Jour. Cosmol. Astropart. Phys.*, 006(02), 2015.
- [70] R Core Team. *R: A Language and Environment for Statistical Computing*. R Foundation for Statistical Computing, Vienna, Austria, 2013.